Structural Interaction of Cytoskeletal Components

MANFRED SCHLIWA and JONATHAN van BLERKOM
Department of Molecular, Cellular and Developmental Biology, University of Colorado, Boulder,
Colorado 80309. Dr. Schliwa's present address is the Laboratory of Molecular Biology, University of
Wisconsin, Madison, Wisconsin 53706.

ABSTRACT   Three-dimensional cytoskeletal organization of detergent-treated epithelial African green monkey kidney cells (BSC-1) and chick embryo fibroblasts was studied in whole-mount preparations visualized in a high voltage electron microscope. Stereo images are generated at both low and high magnification to reveal both overall cytoskeletal morphology and details of the structural continuity of different filament types. By the use of an improved extraction procedure in combination with heavy meromyosin subfragment 1 decoration of actin filaments, several new features of filament organization are revealed that suggest that the cytoskeleton is a highly interconnected structural unit.

   In addition to actin filaments, intermediate filaments, and microtubules, a new class of filaments of 2- to 3-nm diameter and 30- to 300-nm length that do not bind heavy meromyosin is demonstrated. They form end-to-side contacts with other cytoskeletal filaments, thereby acting as linkers between various fibers, both like (e.g., actin-actin) and unlike (e.g., actin–intermediate filament, intermediate filament–microtubule). Their nature is unknown. In addition to 2- to 3-nm filaments, actin filaments are demonstrated to form end-to-side contacts with other filaments. Y-shaped actin filament "branches" are observed both in the cell periphery close to ruffles and in more central cell areas also populated by abundant intermediate filaments and microtubules. Arrowhead complexes formed by subfragment 1 decoration of actin filaments point towards the contact site. Actin filaments also form end-to-side contacts with microtubules and intermediate filaments. Careful inspection of numerous actin-microtubule contacts shows that microtubules frequently change their course at sites of contact. A variety of experimentally induced modifications of the frequency of actin-microtubule contacts can be shown to influence the course of microtubules. We conclude that bends in microtubules are imposed by structural interactions with other cytoskeletal elements.

   A structural and biochemical comparison of whole cells and cytoskeletons demonstrates that the former show a more intricate three-dimensional network and a more complex biochemical composition than the latter. An analysis of the time course of detergent extraction strongly suggests that the cytoskeleton forms a structural backbone with which a large number of proteins of the cytoplasmic ground substance associate in an ordered fashion to form the characteristic image of the "microtrabecular network" (J. J. Wolosewick and K. R. Porter. 1979. J. Cell Biol. 82:114-139).

It is now well established that most animal cells contain ordered arrays of three major fiber systems: microtubules, microfilaments, and intermediate filaments. Their organization in different cell types has been extensively studied at the light microscope level with immunochemical procedures (for reviews, see references 4, 12, 38). In addition, efforts have been made to visualize a cell's skeleton at the electron microscopic level. In recent years, a technique for sample preparation that circumvents embedding, namely, whole-mount electron mi-

croscopy, has become increasingly attractive. When this technique is combined with a method for the detergent extraction of less stable cytoplasmic components, the remaining filament structures are readily visualized. Earlier approaches used negative staining to examine the "detergent-resistant cytoskeleton" (5, 21, 30, 40), but under these conditions information on the three-dimensional organization is lost. However, if combined with critical point drying from CO_2, scanning electron microscopy (16, 36) or transmission electron microscopy (14, 18, 41)

reveals cytoskeletal organization in its three-dimensionality. A different approach has been chosen by Heuser and Kirschner (15) and Batten et al. (2) who used rapid freezing and rotary shadowing to generate replicas in which they studied filament organization in extracted cells. This procedure gives images of outstanding quality and high information value because it provides excellent resolution at the supramolecular level. However, due to the metal coating required in replica formation, it also has the disadvantage that details are observable to only a limited depth; in essence, these preparations allow perusal of a depth corresponding roughly to that of a thin section.

Although some of the published reports do demonstrate good preservation of three-dimensionality (see especially references 14, 15), we thought that high voltage electron microscopy in conjunction with improved extraction techniques might reveal additional insights into the cytoskeletal organization of cells and, most especially, of the structural continuity of different filament types. Also, such an approach would allow a comparison of detergent-treated cells and intact unextracted cells previously studied by high voltage electron microscopy (6, 7, 44, 45). Such a comparison might not only answer some questions pertinent to the three-dimensional organization of intact cells but also clarify the effects of the extraction process. In the search for an extraction buffer that results in excellent preservation of all three major fiber systems, we tested several buffers reported in the literature, as well as a large number of additional variations. Using stereo electron microscopy, we have analyzed the three-dimensional organization of cells extracted under these various conditions. We have identified a simple buffer system which, in our hands, gives excellent morphological results in detergent extraction experiments. With this buffer, we have obtained morphological evidence for extensive structural interaction between various cytoskeletal components.

MATERIALS AND METHODS
Cell Culture

African green monkey kidney cells (strain BSC-1) were cultured in Dulbecco's Minimal Essential Medium supplemented with 10% fetal calf serum. Cells trypsinized from flasks were seeded into 35-mm culture dishes containing gold grids attached to a cover slip.

Chick embryo fibroblasts were obtained by dissociating lungs excised from 8- to 10-d-old chick embryos. They were seeded directly into 35-mm dishes and used after 1-2 d of culture.

Cell Extraction and Fixation

We have tested a number of extraction media reported in the literature, including those used by Brown et al. (5), Small and Celis (30), Ben Ze'ev et al. (3), and Osborn et al. (22), plus ~25 additional variations. The factors tested for their influence on the result of extraction included: the concentration of EDTA and magnesium ions, pH, ionic strength, and the presence or absence of stabilizing agents such as polyethylene glycol, dimethylsulfoxide, and glycerol. It turns out that so long as the pH is kept close to neutrality and the ionic strength near or slightly below the physiological, the most critical factor is the concentration of EGTA which, in turn, controls the concentration of free calcium during the lysis step. High EGTA (around 10 mM or more) preserves structural integrity of all fibrous components of the cytoskeleton and makes the use of an agent such as polyethylene glycol or dimethylsulfoxide superfluous. On the basis of an analysis of hundreds of stereo pairs, we have identified a simple buffer that works best for our purposes. It contains 60 mM 1,4 piperazine diethylsulfonic acid (PIPES), 25 mM N-2-hydroxyethylpiperazine N1-2-ethanesulfonic acid (HEPES), 10 mM EGTA, and 2 mM $MgCl_2$, pH 6.9 (PHEM buffer) (25). This buffer has been employed as our basic extraction buffer in most of the experiments. In a typical extraction experiment, cells were briefly washed with PHEM buffer and then lysed with PHEM buffer supplemented with 0.15% Triton X-100 for 1-1.5 min,

fixed with 1% glutaraldehyde in PHEM buffer, washed in buffer, and postfixed with 0.5% OsO_4 for 1-2 min.

Extraction of actin and associated proteins was achieved by treatment of Triton-extracted cells with buffers of low and high ionic strength similar to those described by Small and Sobieszek (31). The buffers contained 1 mM EDTA, 2 mM EGTA, 1 mM cysteine, 5 mM ATP, 25 mM PIPES (pH 7.0), and either 60 mM KCl (low ionic strength buffer) or 600 mM KCl (high ionic strength buffer). Cells were treated for at least 10 min with each buffer in the order low-high-low ionic strength. To stabilize microtubules normally extracted during this treatment, Taxol (24) has been added to the Triton extraction medium at a concentration of 1 μg/ml. In another set of experiments, intermediate filaments were extracted with a 5-min treatment of 0.1% Sarkosyl (5) in PHEM buffer. In these experiments, actin filaments were stabilized by a 2- to 3-min treatment with Phalloidin (43) at 10 μg/ml before the sarkosyl extraction. Polyacrylamide gel electrophoresis (PAGE) demonstrates actin or vimentin (the intermediate filament protein of BSC-1 cells), respectively, to be the predominant polypeptide species remaining in the cytoskeleton under the two sets of extraction conditions.

Decoration with Heavy Meromyosin Subfragment 1

Heavy meromyosin subfragment 1 (S1), a generous gift of Dr. Frank Pepe, University of Pennsylvania, Philadelphia, Pa., was prepared from chicken myosin according to the method of Weeds and Taylor (42). For S1 decoration, Triton-extracted cells were treated with S1 (~1 mg/ml) in PHEM buffer supplemented with 20% glycerol for 1-1.5 min, washed twice with buffer, and fixed with 1% glutaraldehyde plus 0.4% tannic acid in PHEM buffer. After a brief buffer wash, cells were postfixed with 0.5% OsO_4 for 3 min.

Cytochalasin Treatment

Cytochalasins B and D (Sigma Chemical Co., St. Louis, Mo.) were kept as stock solutions of 1 mg/ml at $-20°C$. Cells were treated with 5 μg/ml cytochalasin B or D in culture medium at 37°C for 15-30 min. Control preparations received 0.5% DMSO, a concentration that did not affect cell morphology or cytoskeletal organization.

Preparation of Microtubule Protein and Microtubule Assembly In Vitro

Microtubule protein was isolated from bovine brain by three cycles of temperature-dependent assembly and disassembly according to the method of Shelanski et al. (29). Aliquots of cycle-3 microtubule protein were assembled at 37°C. A small drop of this preparation was applied to an electron microscopic grid, fixed with glutaraldehyde and OsO_4, dehydrated, and critical point dried (see below).

High-speed supernates (HSS) were prepared by the spinning of an aliquot of microtubule protein at 250,000 g for 3 h. The supernate of this spin exhibits reduced capacity for self-nucleated microtubule assembly. HSS at a concentration of 0.5 mg/ml was added to Triton-extracted cells on cover slips, and the preparations were incubated at 25°C for 40 min. The HSS solution was washed off, and the cells were fixed and processed for immunofluorescence microscopy.

Immunofluorescence Microscopy

Cells were fixed for immunofluorescence microscopy with 0.5% glutaraldehyde in PHEM buffer, washed with buffer, and then treated with $NaBH_4$ (1 mg/ml), first in PHEM buffer and then in phosphate-buffered saline (39). After two additional washes, cells were incubated at 37°C for 45 min with a tubulin antiserum generously provided by Dr. Keigi Fujiwara, Harvard Medical School, Boston, Mass. (8). After thorough washes with phosphate-buffered saline, cells were reacted with fluoresceine-conjugated goat-anti-rabbit immunoglobulins (Miles Laboratories, Inc., Miles Research Products, Elkhart, Ind.) for 30-45 min. Cover slips were mounted on slides and viewed in a Leitz Orthoplan light microscope equipped with epifluorescence illumination.

High Voltage Electron Microscopy

The methods of cell preparation for high voltage electron microscopy have been described previously (44, 45). Briefly, cells are grown on gold grids sandwiched between a carbon-coated Formvar film and a glass cover slip. After experimental treatment and fixation (see Cell Extraction above), cells are dehydrated in ethanol and critical point dried from CO_2 in a Sorvall critical point drier (DuPont Instruments-Sorvall, DuPont Co. Newtown, Conn.) A thin film of

carbon is then evaporated onto the specimen to increase stability in the electron beam. The cells are viewed in a Jeol high voltage electron microscope operated at 1,000 kV.

Isotopic Labeling and Two-Dimensional PAGE

Cell cultures were labeled with [^{35}S]1-methionine (1,000 Ci/mmol sp act, New England Nuclear, Boston, Mass.) at a concentration of 300 μCi/ml for 2 h. After radiolabeling, cells were washed twice in PHEM buffer (without Triton) and harvested with a rubber policeman. Labeled cells were pelleted by low-speed centrifugation and then lyophilized. Other cell cultures were exposed to extraction buffer for 1.5 min. Cellular material remaining after extraction was collected with a rubber policeman, centrifuged, and lyophilized. Immediately following lyophilization, samples were resuspended in lysis buffer (20) and subjected to isoelectric focusing electrophoresis.

Two-dimensional PAGE was accomplished according to the procedures of O'Farrell (20). Linear gradient slab gels were prepared as previously described (37). Approximately 1.5 × 10^6 cpm of incorporated radioactivity was applied to the first-dimension gel. Exposure to x-ray film lasted for 12 h.

RESULTS

Overview of the Cytoskeletal Organization of Chick Embryo Fibroblasts and BSC-1 Cells

Chick embryo fibroblasts and BSC-1 cells extracted with 0.1% Triton X-100 in PHEM buffer completely retain their three-dimensional organization. No change whatsoever in cell morphology during extraction is detectable in phase-contrast microscopy with a × 63 objective. An analysis of the time-course of Triton extraction shows that part of the plasmalemma is already removed within 5 s after immersion in the detergent; the entire plasmalemma, many of the components of the cytoplasmic ground substance, and membranes of internal organelles such as the endoplasmic reticulum and mitochondria are extracted after 10-20 s. The stereo pair seen in Fig. 1 illustrates in an overview the structural organization of a fibroblast extracted for 40 s. This cell, and others extracted under similar conditions, displays three major cytoskeletal domains characterized by distinctly different arrangements of various fibers: (a) filament bundles (stress fibers) predominantly near the substrate surface, (b) ruffles at the cell periphery, and (c) a loose fiber network extending throughout the cell proper. The cytoskeletal organization of epithelial BSC-1 cells differs from that of chick embryo fibroblasts mainly in two aspects: ruffles are not very prominent, and the three-dimensional fiber network extending throughout the cell body appears much denser (Fig. 2).

In both BSC-1 cells and fibroblasts, the filament network overlying substrate-associated filament cables appears to be composed of single filaments, not bundles (Fig. 3). These filaments fall into three different size classes: 9-11 nm, 6-8 nm, and 2-3 nm. Microtubules with a diameter of ~20 nm are easily distinguished from these filaments. Their smaller than usual diameter indicates some shrinkage probably induced by the critical point drying (see references 14, 34). Both microtubules and filaments are of uniform diameter throughout their length.

All filament types are observed to be associated with one another and with microtubules in one of two possible ways: (a) lateral association: filaments are in contact with their surfaces in a crossover pattern; and (b) end-to-side association: the end of one filament is in contact with the surface of another, resulting in a triangular pattern. These associations will be described in more detail below.

Ruffles of both chick embryo fibroblasts and BSC-1 cells consist of a tightly woven network of filaments with a diameter

of 6-8 nm. Frequently, the dense mesh extends in two dimensions only, forming a sheetlike structure protruding from the front end of the cell (Fig. 1). Crossover points of filaments frequently appear thickened. Ruffles are not sharply separated from the loose filament network of the main cell body; rather, there exists a transition zone in which interfilament spaces gradually enlarge and the distance between crossover points of filaments increases. Microtubules, 9- to 11-nm filaments, and 2- to 3-nm filaments are absent from ruffles.

Architecture of the Cytoskeleton

SELECTIVE EXTRACTION OF DIFFERENT COMPONENTS: To obtain an overview of the distribution and spatial organization of actin filaments alone, we extracted intermediate filaments, microtubules, and 2- to 3-nm filaments with the ionic detergent Sarkosyl while stabilizing F-actin with phalloidin (Fig. 4). The three-dimensional organization of actin filaments appears to be well preserved. Filament bundles extend the long axis of the cell, passing both underneath and over the nuclear remnant. As in cytoskeletons before sarkosyl extraction, ruffles show a dense network of filaments whose overall three-dimensional structure is not appreciably affected by sarkosyl extraction.

Visualization of intermediate filaments alone involved the removal of actin and associated proteins as well as microtubules with buffers of low and high ionic strength (31). As a rule, the cytoskeletons tended to detach from the substrate under these extraction conditions, a problem we have overcome by coating the grids with poly-L-lysine before plating of the cells. Fig. 5 shows the organization of intermediate filaments in BSC-1 cells. In this cell type, as in chick embryo fibroblasts, filaments form a loose network in which interfilament spaces may be wider in some areas than in others; filament bundles are never observed. This is in marked contrast to PtK1 cells where, in addition to a network of single filaments, wavy filament bundles are prominent (not shown). Interestingly, filament ends are rarely observed, indicating that individual filaments may be very long.

Architecture of the Cytoskeleton

DECORATION OF ACTIN FILAMENTS WITH HMM-S1: The visualization of a specific filament type is of value only for the study of its overall distribution and arrangement. Because cross-connections between different cytoskeletal components apparently exist (Fig. 3), the removal of certain structural elements can be expected to result in disturbances of the arrangement of the remaining filament type. Ideally, one should be able to analyze fine details of cytoskeletal organization and at the same time identify and distinguish different filament types on the basis of characteristic morphological markers. Antibody decoration has yielded good results (14, 41), but details may be obscured or certain components (such as microtubules) may be lost according to the procedures employed. We have used S1 to decorate actin filaments with periodic arrowheads to allow an easier distinction from 2- to 3-nm filaments and intermediate filaments. As demonstrated in Fig. 6, the rapid procedure of S1-decoration employed does not cause any detectable distortion of the three-dimensional organization of extracted cells. At higher magnification (Fig. 7), the extensive interconnection of different cytoskeletal structures is made readily visible. Of particular interest is the role played by the 2- to 3-nm filaments and actin. The former appear to be true linkers or bridge structures which intercon-
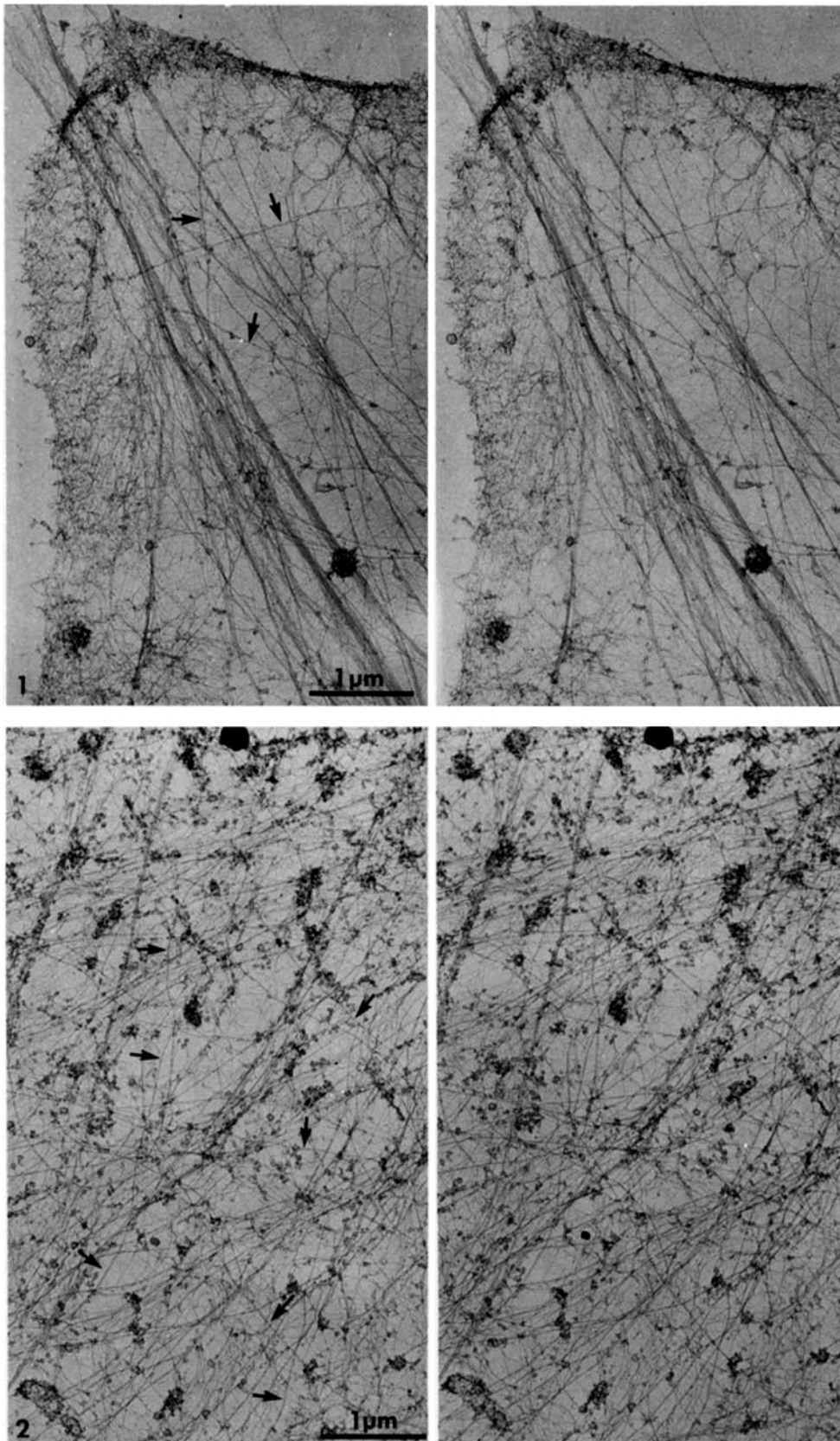
FIGURE 1   Leading edge of a chick embryo fibroblast extracted with Triton X-100 for 40 s. This stereo pair illustrates the main aspects of cytoskeletal organization in this cell type. Its most conspicuous feature is the dense mat of filaments forming the ruffle. Overlying substrate-associated bundles of filaments (stress fibers) is a loose filament meshwork in which microtubules (arrows) are suspended. The loose filament mesh extending throughout the cell proper gradually merges into the dense network present in the ruffle. × 17,500.

FIGURE 2   Epithelial BSC-1 cell extracted under similar conditions as the chick embryo fibroblast shown in Fig. 1. Several small filament bundles are present near the substrate side of the cell. The three-dimensional filament network extending throughout the cell appears denser than in comparable areas of chick embryo fibroblasts. Numerous microtubules (arrows) can be seen to curve through this network. Many ribosomes are still associated with the cytoskeleton. × 17,500.
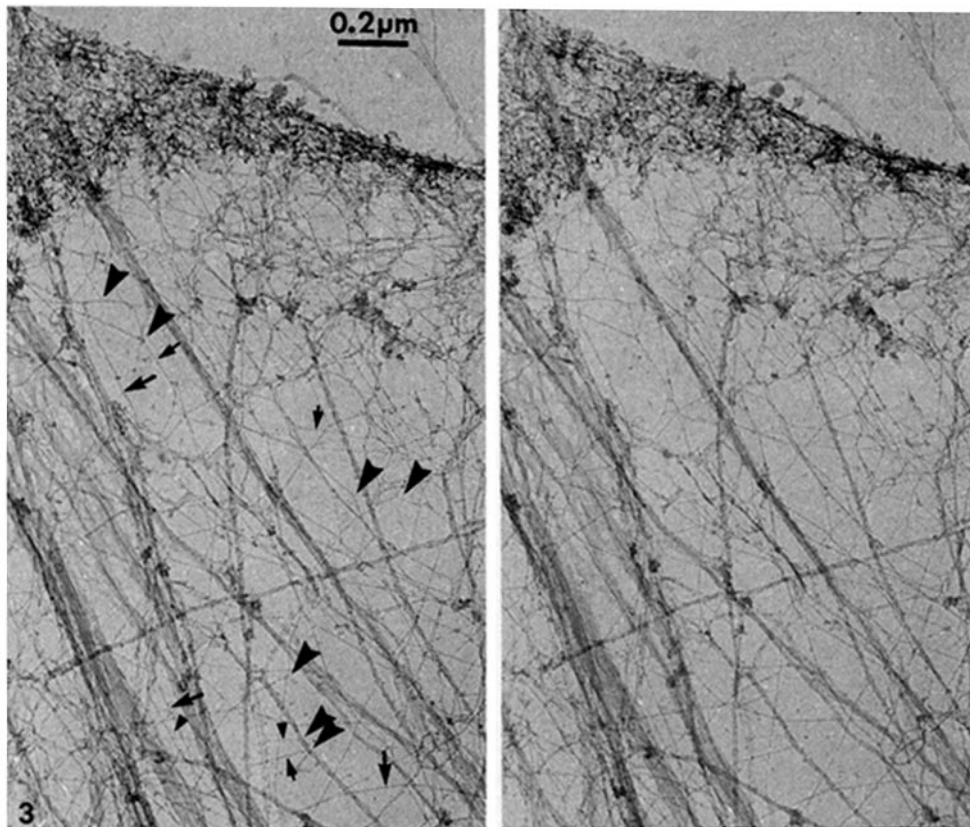
FIGURE 3   Higher magnification of part of Fig. 1. Three different filament types can be seen to form the three-dimensional fiber network: 9- to 11-nm filaments (large arrows), 6- to 8-nm filaments (small arrows), and 2- to 3-nm filament (arrowheads). There are numerous connections of these filaments with one another, including end-to-side contacts (large arrowheads). × 42,000.

nect both like (e.g., actin-actin) and unlike (e.g., actin-microtubule) filament types. [4]

Apart from 2- to 3-nm filaments, only actin filaments are observed frequently to form end-to-side contacts with other cytoskeletal structures. Actin-actin connections appear as a Y-shaped "branch." Such contacts are most frequent in the cell periphery close to ruffles (Figs. 8 and 9). According to the high filament density in the ruffle itself, identification of bifurcating contact patterns is virtually impossible in this structure. F actin "branches" are also encountered, however, in more central cell areas also populated by abundant microtubules and intermediate filaments. Most interestingly, actin filaments form end-to-side contacts with these cytoskeletal elements as well (Fig. 10). At contact points with microtubules, the latter frequently change their direction as if tension is applied to microtubules by some other component(s), as discussed below. Between contacts, microtubules maintain a straight course. S1-decorated actin filaments connected to another cytoskeletal component, whether it is a microtubule, an intermediate filament, or another actin filament, have their arrowheads pointing towards the contact site; this observation is based on an analysis of several hundred micrographs.

Lateral contacts between different filament types are at least as frequent as end-to-side connections. It is difficult, however, to decide whether the filaments are firmly linked together (e.g., by specific cross-linking proteins), or whether they are merely in close apposition without specific interaction.

Modification of the Frequency of Actin-Microtubule Contacts

The observation of actin filament contacts with the surface

of microtubules and their apparent influence on the course of microtubules suggests that the curvilinear paths of microtubules in cells (Fig. 11) may be influenced by structural interaction with other components. This possibility led us to investigate the effect of experimental manipulations on the frequency of filament-microtubule contacts. The following experiments were performed to test whether directional changes in microtubules are imposed by external forces.

(a) The assembly of tubulin onto the ends of preexisting cellular microtubules: high-speed supernates of porcine brain microtubule protein assembles onto the ends of cellular microtubules in Triton-extracted cells, thereby elongating the preexisting cellular microtubules beyond the cell margin. Added microtubule segments which, in the extracellular space, do not have a chance to interact with other structures maintain a straight course (Fig. 12). (b) In vitro reassembly of microtubules: microtubules assembled in vitro from brain microtubule protein, if applied to a grid and critical point dried (not negatively stained), appear as straight tubes which change their direction only if in contact with another microtubule or the substrate (not shown). (c) Removal of actin filaments from Triton-extracted cytoskeletons: actin filaments are removed form cytoskeletons by a high ionic strength buffer. We took advantage of the properties of Taxol (24) to stabilize microtubules during this treatment. Intermediate filaments and microtubules are the only fibrous components remaining. Removal of actin filaments, and, hence, elimination of F actin–microtubule contacts (Table I), causes the microtubules to assume a straight course over relatively long distances (Fig. 13). Directional changes are imposed only by occasional contacts with intermediate filaments or other microtubules. (d) Actin network disruption in vivo: cells treated with 5 μg/ml cytochalasin
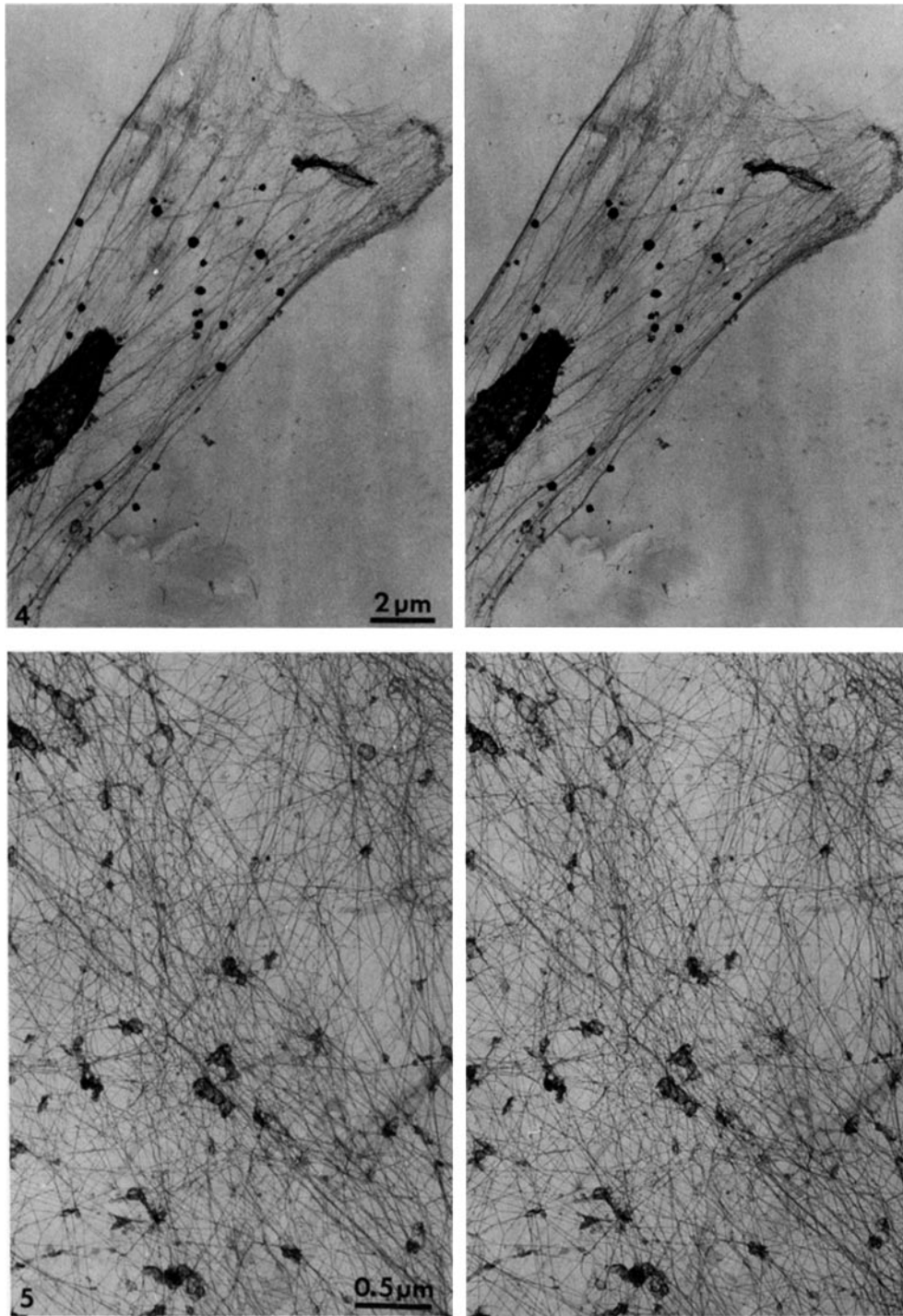
FIGURE 4   Chick embryo fibroblast extracted with sarkosyl to demonstrate the overall arrangement of actin filaments. Filament bundles pass both over and under the nuclear remnant. Some dense granules are still associated with the actin cytoskeleton. × 4,500.

FIGURE 5   BSC-1 cell extracted with low and high ionic strength buffers to remove actin and associated proteins. The cytoskeletal remnant consists only of 9- to 11-nm filaments. This micrograph is taken from an area close to the nucleus where filament density is highest. × 20,000.

D or B for 15–30 min, followed by extraction with Triton, show a severe disruption of the filamentous network, including a substantial reduction of the frequency of F actin–microtubule connections (Table I). As in the preceding in vitro experiment, the relative proportion of straight microtubule segments increases (Fig. 14).

Comparison with Intact Cells

A structural comparison between intact and Triton-extracted whole-mount preparations of BSC-1 cells reveals that many of the fibrous elements comprising the so-called "microtrabecular network" (44) of unextracted cells have been removed upon
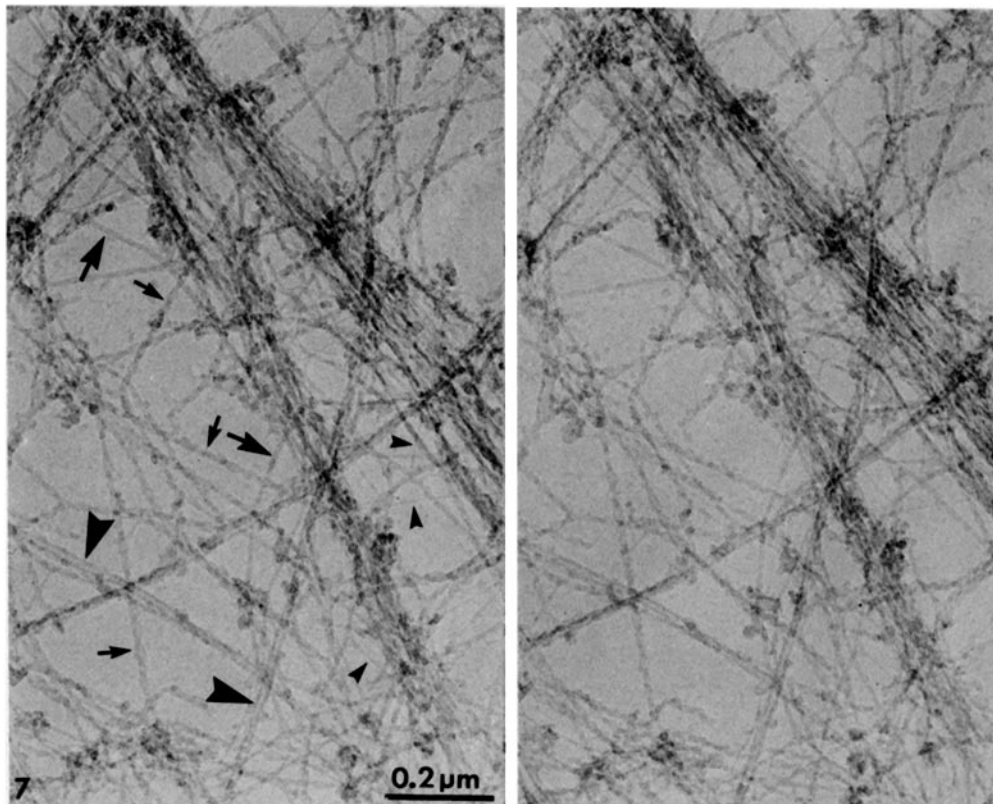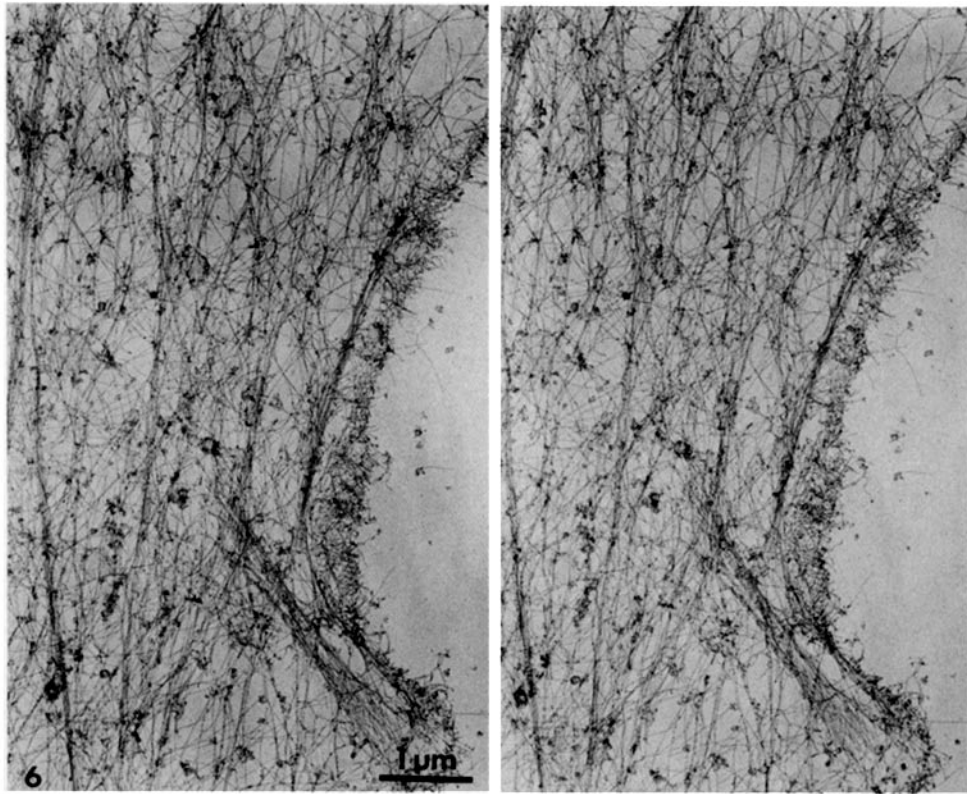
FIGURE 6   Part of the cell periphery of a BSC-1 cell labeled with heavy meromyosin subfragment 1. With the procedure of S1 labeling employed here, three-dimensional cytoskeletal organization is not disturbed. × 12,000.

FIGURE 7   Higher magnification of a BSC-1 cell labeled with S1. This stereo pair has been included to demonstrate the ease with which the different fiber types, namely, smooth intermediate filaments (large arrows), decorated actin filaments (small arrows), 2- to 3-nm filaments (arrowheads), and microtubules (large arrowheads) can be distinguished. Note that 2- to 3-nm filaments act as linkers between other components of the cytoskeleton. × 70,000.
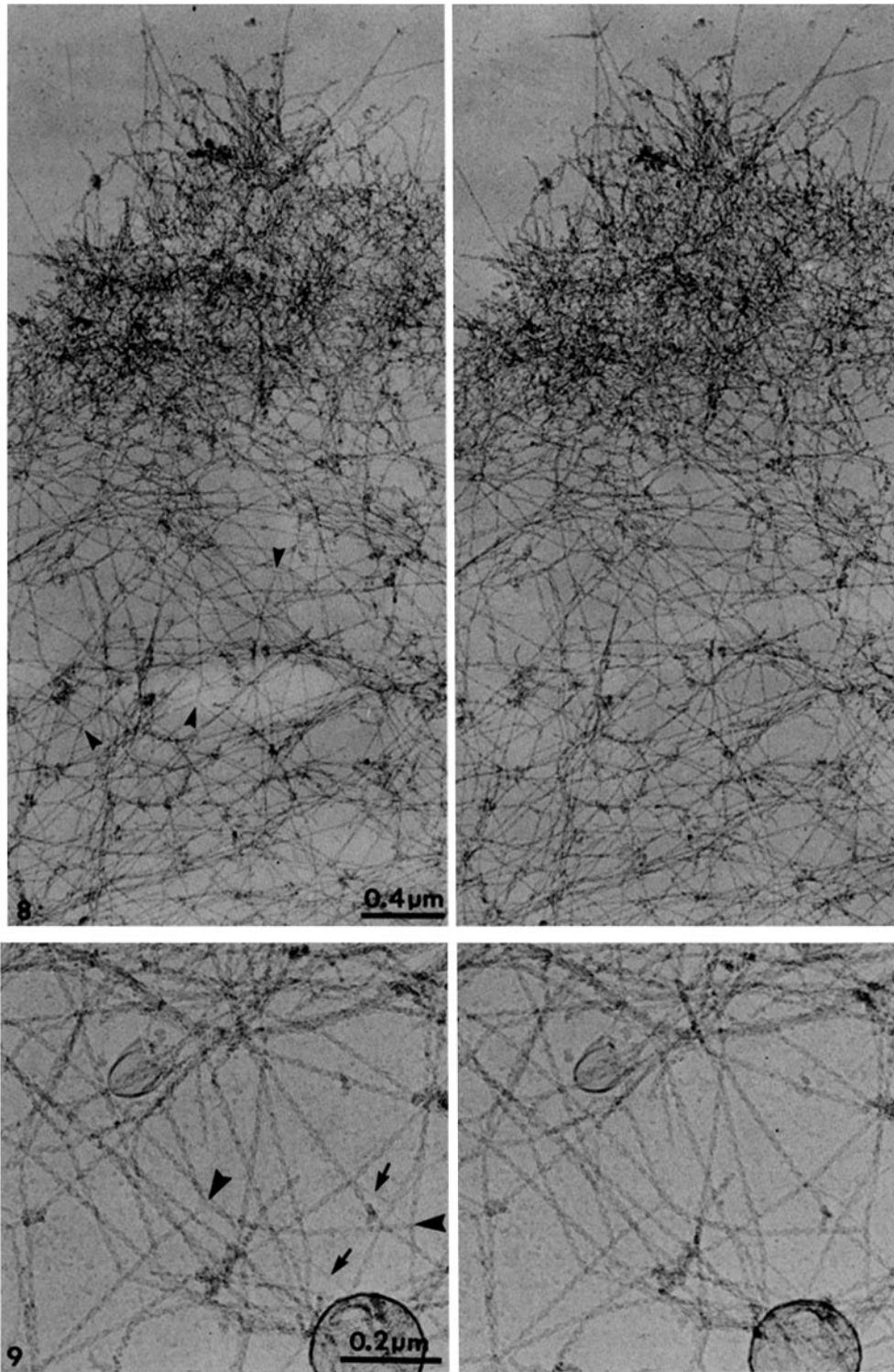
FIGURE 8 Micrograph taken from the cell periphery of an S1-decorated BSC-1 cell. Note how the dense mesh of filaments present in the "mini-ruffle" at the top gradually transforms into a looser network in the more proximal cell area. Several Y-shaped end-to-side contacts or "branches" of actin filaments are denoted by arrowheads. Except for a few 2- to 3-nm filaments, the fiber network consists exclusively of decorated actin filaments. × 31,000.

FIGURE 9 High magnification of an area that includes two end-to-side contacts (arrowheads) of actin filaments. Filament polarity can easily be recognized according to the orientation of arrowheads. Actin filaments in contact with another actin filament have their arrowheads pointing towards the site of contact. Some 2- to 3-nm filaments are denoted by small arrows. × 70,000.
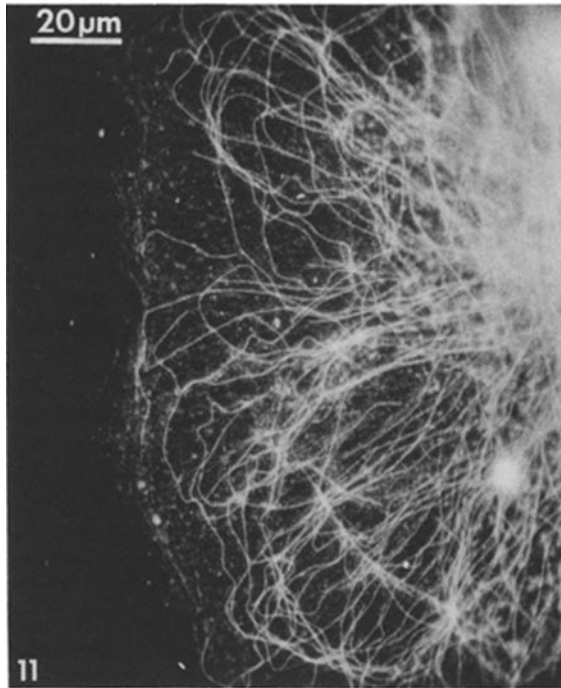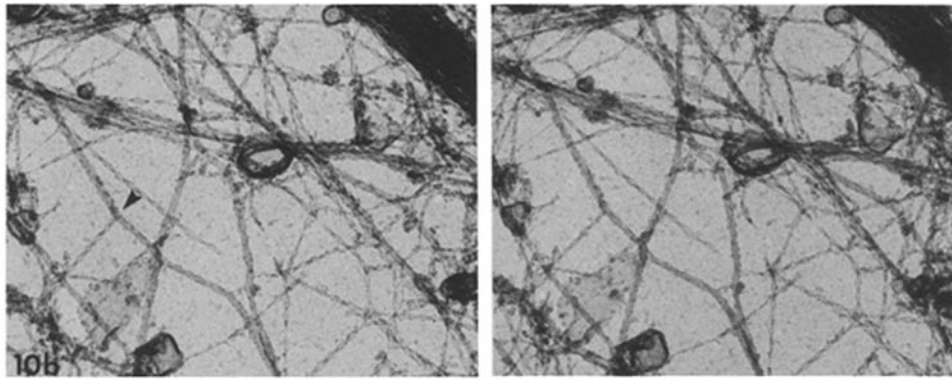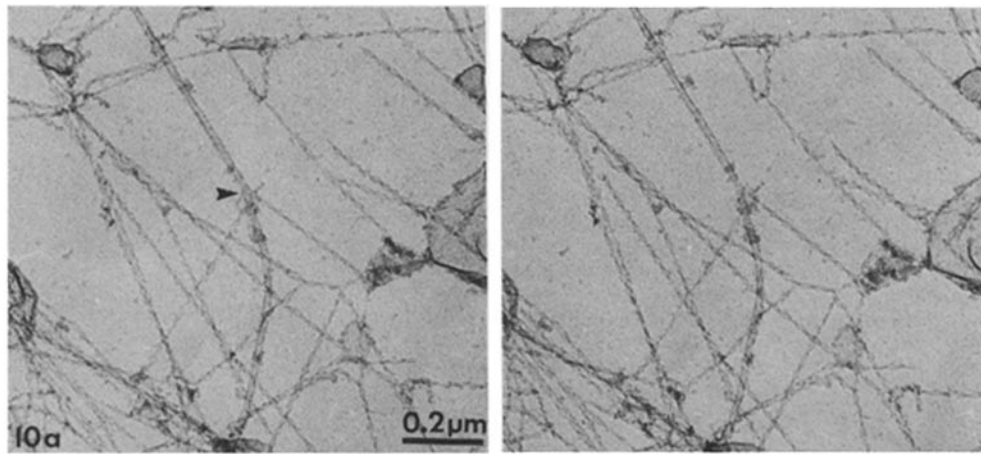
FIGURE 10 (*a* and *b*) Two examples of end-to-side contacts of actin filaments with microtubules. S1-arrowheads point towards the contact side. The area shown in *b* was photographed at 100 kV. × 52,000.

FIGURE 11 Microtubule pattern of BSC-1 cell as seen in indirect immunofluorescence microscopy with tubulin antibodies. Note the waviness and curvilinear pathways of individual microtubules. × 600.

FIGURE 12 Triton-extracted BSC-1 cell treated with 0.5 mg/ml of a high speed supernate of a brain microtubule protein preparation for 40 min at 25°C in a buffer containing 100 mM PIPES, 1 mM MgCl₂, 1 mM EGTA, 2 mM GTP, pH 6.9. Cells were then fixed and processed for immunofluorescence microscopy. Cellular microtubules have elongated beyond the cell margin. Newly formed microtubule segments (arrowheads) are straight. × 600.

Treatment	Number of contacts/ μm
Untreated	5.6 ± 1.7
Low and high ionic strength	1.8 ± 1.1
20-min cytochalasin D (5 μg/ml)	2.7 ± 1.9

The number of contacts of other cytoskeletal structures with microtubules was scored in stereo electron micrographs taken from equivalent cell areas. In each experiment, the number of contacts along ~100-μm microtubule length was determined. Their frequency is given as mean ± SD. For explanation of experimental conditions, see text.

lysis (Fig. 15 a and b). The Triton-stable cytoskeleton displays a more open filament arrangement in which inter-fiber spaces are larger. The apparent loss of structural components is paralleled by a dramatic reduction in the number of polypeptides in the cytoskeleton, as revealed by two-dimensional gel electrophoresis of [^{35}S]methionine-labeled cellular proteins (Fig. 15 c and d). Major constituents of extracted BSC-1 cells include actin, tubulin, and a protein of ~57,000 daltons (vimentin) that comprises intermediate filaments. However, in addition to these proteins, the cytoskeleton includes more than 100 major and minor polypeptides, most of which are as yet unidentified.

Although, as demonstrated in Fig. 15, the structural organization of whole, unextracted, and Triton-extracted cells is rather different, intermediate stages of extraction indicate that the Triton-stable cytoskeleton is part of the "microtrabecular lattice" of whole cells. If BSC cells are immersed in 0.1% Triton for 10 s only, the plasmalemma is largely removed, but only some of the less stable cytoplasmic components have dissolved (Fig. 16). Such preparations reveal a loose network of uniform filamentous structures underlying the more fragile and partly distorted or extracted components of the cytoplasmic ground substance.

DISCUSSION

Using an improved extraction method, we have analyzed the three-dimensional arrangement of filamentous components in cytoskeletons at both low and high levels of resolution. The procedure employed here (a) results in good preservation of all major cytoskeletal fibers, (b) allows their identification both without and, more conveniently, with a morphological marker, and (c) permits an analysis of their structural interrelationships. Heavy meromyosin-S1 labeling has been performed in a way that introduces little, if any, changes in the supramolecular organization of the cytoskeleton; <3 min elapsed between lysis of a cell, S1-labeling, and glutaraldehyde fixation. The essential ingredient of the extraction buffer used here probably is the high EGTA concentration. We assume that it is the Ca^{2+}-chelating activity of this compound and not some unknown cross-linking property that makes it so effective. High EGTA concentrations are essential during the initial phase of lysis only; cytoskeletons may later be transferred to low EGTA media without detrimental effects (28). Possibly, Ca^{2+} ions released from intracellular stores during lysis are chelated rapidly enough to prevent activation of Ca^{2+}-dependent factors affecting cytoskeletal structures (e.g., calmodulin, gelsolin, etc.).

This study demonstrates a surprisingly high degree of structural interaction in the cytoskeleton. Two components seem to be particularly important: the 2- to 3-nm filaments and actin. Filaments with a diameter of 2-3 nm have not yet been described as a regular feature of extracted cells, although structures of a similar morphology have occasionally been noted (e.g., references 1, 23, 35, 41). We found them in all tissue culture cell types examined as linkers between other fibers. They are present in unlabeled and S1-labeled cytoskeletons, but are extracted by sarkosyl, high ionic strength buffers, or KI (not shown). Although they are a minor component by mass, their apparent role as a crosslinker makes these filaments an important component in cytoskeletal consolidation. So far, nothing is known about their chemistry. Their diameter is similar to that of filamin or myosin rods; their length, however, is highly variable, ranging from 30 to 300 nm.

Even more significant as cytoskeletal "integrators" than the 2- to 3-nm filaments are actin filaments. Not only are actin filaments in lateral contact with microtubules or intermediate filaments, but they also form end-to-side contacts with all fiber types. The existence of actin-actin connections in cells in the form of a Y-shaped "branch" has not been clearly demonstrated before. Their visualization has been facilitated through the use of stereo high voltage electron microscopy in conjunction with S1-labeling. It is unlikely that branches have been artifactually produced upon S1 decoration because they are also present, though less readily seen, in undecorated cytoskeletons. Filaments branching from another filament have their arrowheads pointing towards the contact site, meaning that the fast-growing or barbed end (46) is distal. Although Y-shaped branching patterns have also been found in preparations of pure actin, they appear to be rather fragile (19). It is likely, therefore, that the contacts described here are mediated by specific molecules. Recently, Hartwig et al. (13) demonstrated actin filament "branching" in vitro induced by macrophage actin binding protein, and Condeelis (personal communication) has isolated a protein from *Dictyostelium* amoebae with similar properties. Proteins with a similar function have yet to be identified in other cell types, but a widespread occurrence of such proteins seems likely. The specific role of actin filament "branching" for certain cellular activities such as locomotion, ruffling, or organelle transport has yet to be evaluated. However, "branching" can be expected to increase viscosity and influence cytoplasmic consistency.

It is not yet known whether the intact cell contains a substantial amount of F actin that is not bound into the Triton-stable cytoskeleton. If this were not the case, i.e., if the filaments present in the Triton residue represent the entire pool of polymerized actin, then this would lend support to Kirschner's (17) idea that filaments with both ends free are "treadmilled away." At present, it is unknown whether actin removed by Triton is all in a nonpolymerized state or contains a substantial proportion of F actin.

Actin-microtubule connections are, in our opinion, the most interesting subclass of structural interactions described here. Again, we can assume that these interactions are mediated by specific molecules, and in fact microtubule-associated proteins have been identified as possible candidates in in vitro studies (11). Whether they are the only linker protein, and whether different types of interaction (lateral vs. end-to-side) are mediated by different linkers, is not yet known.

Of particular interest is the influence that contacts with other filaments have on the course of a microtubule. On the basis of their protein chemistry, microtubules can be envisioned as straight, elastic polymers which lack an intrinsic potential to change their direction of growth, or their course, unless there are changes in the surface lattice of tubulin molecules. The
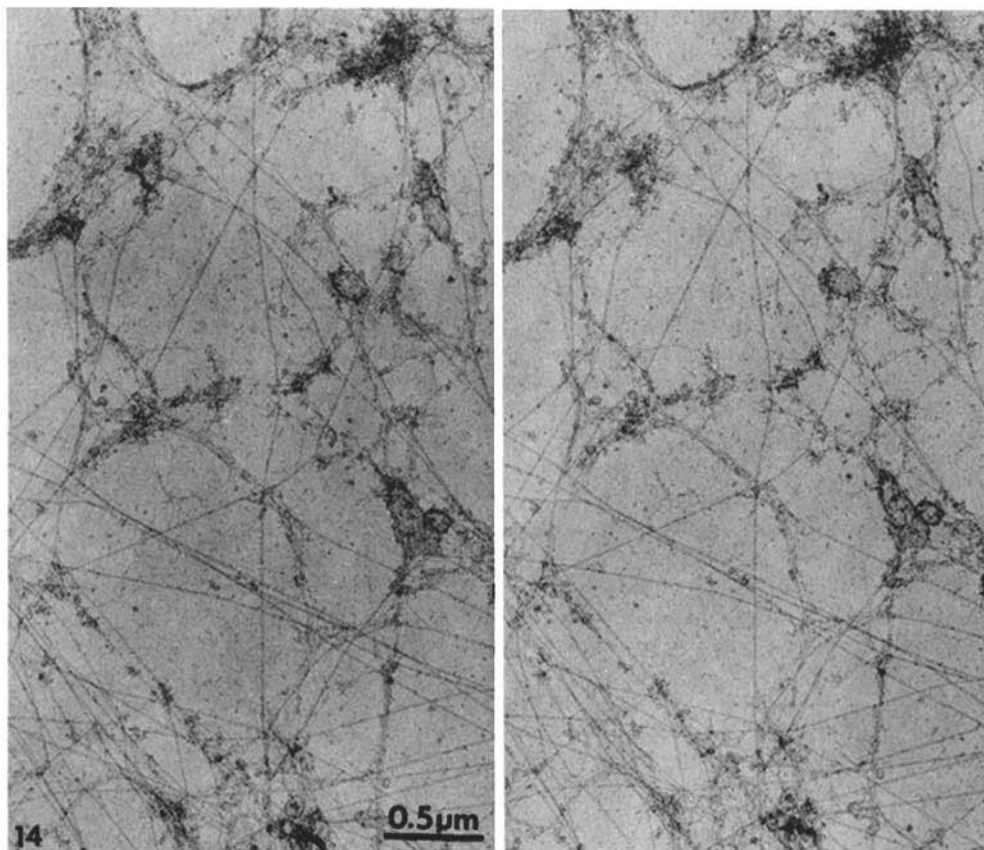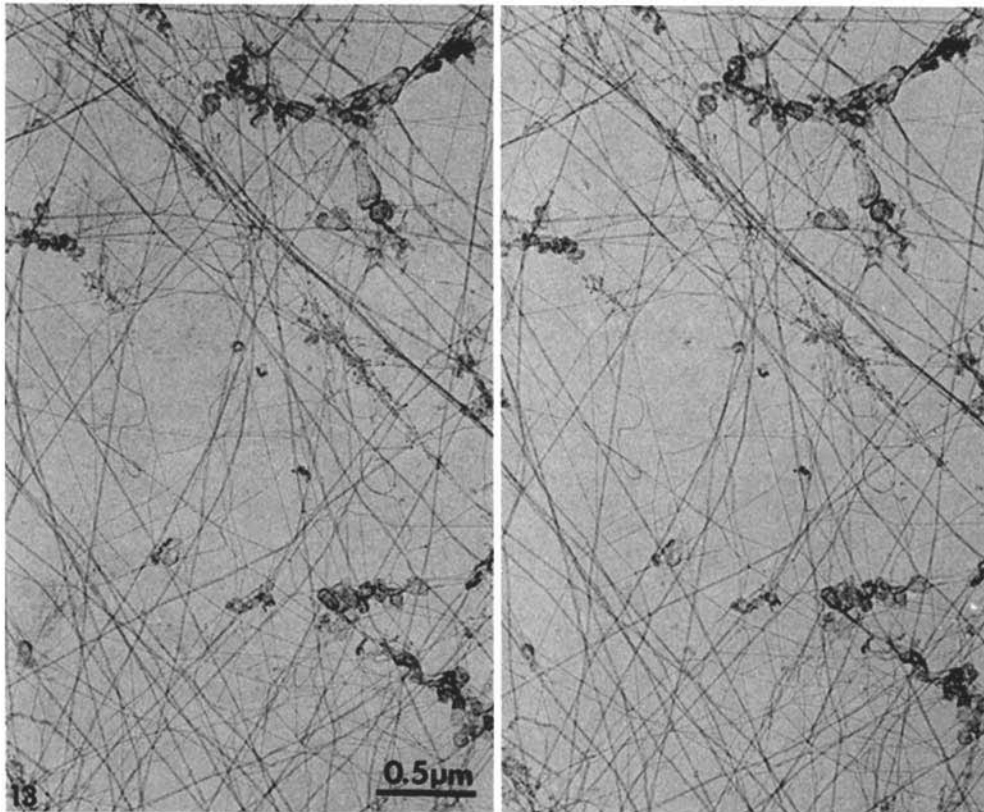
FIGURE 13 Triton-extracted cell treated with low and high ionic strength buffers (see Materials and Methods) after stabilization of the microtubules with Taxol. Intermediate filaments and microtubules are the major fiber structures left. Due to the elimination of actin filaments in contact with microtubules, many of the microtubules assume a much straighter course over relatively long distances. × 25,000.

FIGURE 14 Cytoskeleton of a BSC-1 cell treated with 5 μg/ml cytochalasin D for 20 min. The three-dimensional filament network is severely disrupted. Few contacts of filaments with microtubules have survived this treatment, and many microtubules appear straight over a distance of several micrometers. × 25,000.
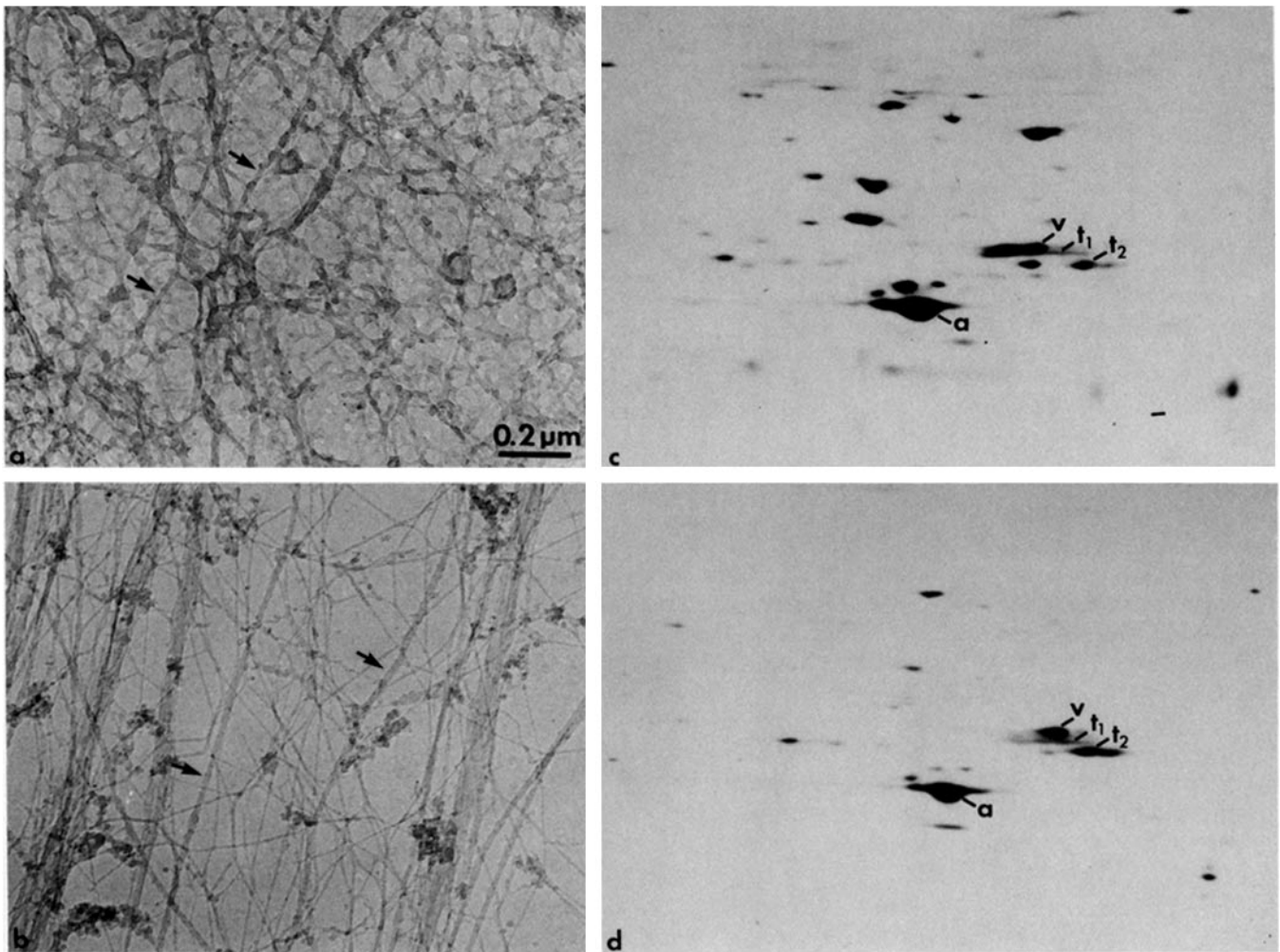
FIGURE 15 Comparison of the structure and polypeptide composition of whole, unextracted and Triton-extracted BSC-1 cells. *a*, part of an unextracted BSC-1 cell, showing the characteristic irregular meshwork organization of the cytoplasm. Arrows = microtubules. × 48,000. *b*, part of a Triton-extracted cell showing the more open network of cytoskeletal fibers. Arrows = microtubules. × 48,000. *c*, two-dimensional PAGE of unextracted BSC-1 cells. Cells were labeled with [^{35}S]methionine at 300 μCi/ml for 2 h; ~1.5 × 10^{6} counts per minute were loaded on the gel. Autoradiographs were exposed for 12 h only to emphasize major polypeptide specie. *a*, actin; t_1, α-tubulin, t_2, β-tubulin, *v*, vimentin. *d*, two-dimensional gel electrophoretic pattern of a cytoskeletal preparation of Triton-extracted BSC-1 cells. Sample preparation as in *c*.

precise and absolutely predictable arrangement of tubulin subunits in the microtubule wall implies that these organelles can grow for microns (or miles, for that matter) without changing their direction of growth. This can nicely be demonstrated by dark-field microscopy of microtubules assembled from microtubule-organizing centers in vitro (32, 33): microtubules are arranged in a precise radial array around the organizing center and individual microtubules are perfectly straight. Microtubule organization in vivo as seen by, e.g., immunofluorescence microscopy, differs markedly from the in vitro pattern just described. In cells, microtubules may curve and bend rather sharply. Because, at present, we have no indication of frequent surface lattice irregularities in microtubules, the phenomenon of their waviness in vivo has to find another explanation. From our experiments we conclude that bends in microtubules are imposed by interaction with other cytoskeletal structures. Microtubules seem to be bound into a dynamic and flexible three-dimensional network of relatively stable filamentous components. It is conceivable that this network is under tension, and

that tension may change locally and transiently, implying that within certain spatial limits the position of a microtubule or part of it may likewise be subject to changes. As a note of caution, it should be mentioned that critical point drying employed here for specimen preparation is likely to induce some shrinkage, thereby possibly exaggerating directional changes at contact points; we are now using other methods of specimen preparation to study the possible influence of preparative techniques on cytoskeletal organization. In any case, the observations suggest that what we call a cell-type-specific microtubule pattern as visualized by, e.g., immunofluorescence microscopy, may, in fact, be determined by a (cell-type-specific?) pattern of interactions with other elements of the cytoskeleton. How these interactions are changed in association with different cellular activities remains to be elucidated.

It is evident from our comparative structural analysis of whole cells and extracted cytoskeletons that the former display a much more intricate three-dimensional network of filamentous structures that the latter. Possibly, the cytoskeleton forms
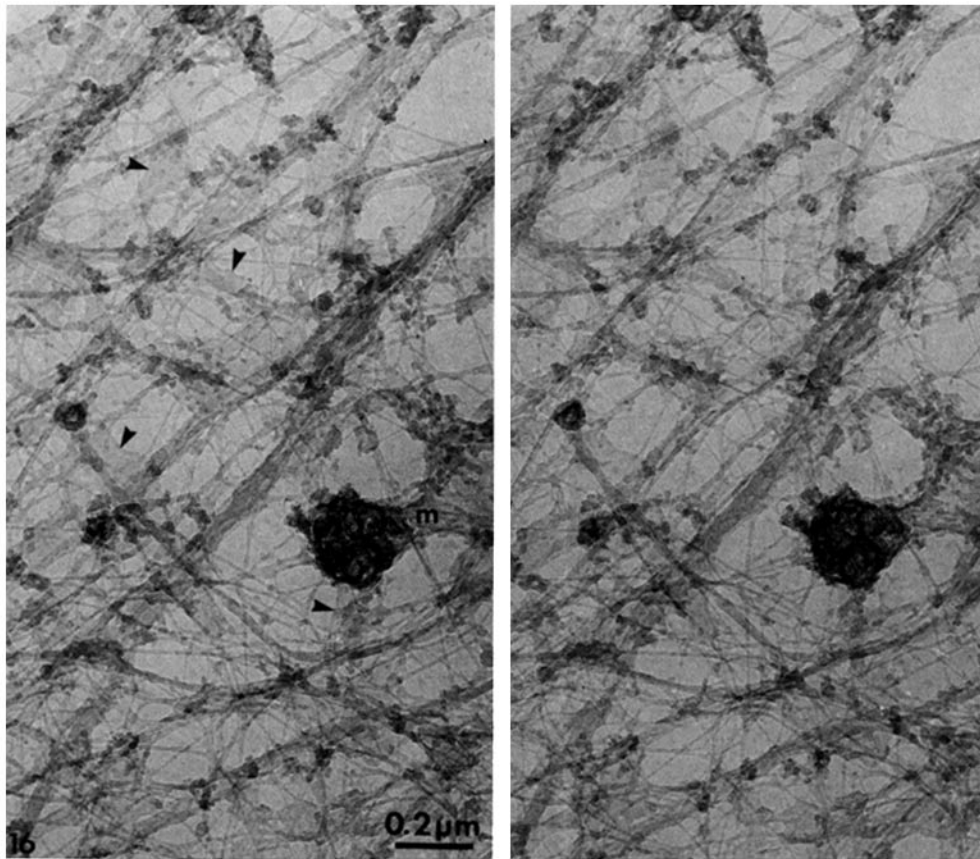
FIGURE 16 Part of BSC-1 cell extracted with Triton X-100 for 10 s only. The process of extraction has been interrupted before completion, but the three-dimensional network of filaments is already beginning to emerge. All the filamentous components of fully extracted cytoskeletons (microtubules, 6-nm [actin] filaments, 10-nm [intermediate] filaments, and 2- to 3-nm filaments) can be identified. However, these structures are frequently studded with lumps or aggregates of irregularly shaped material. M, partly extracted mitochondrion. X 48,000.

a structural backbone with which other proteins of the cytoplasmic ground substance associate in an ordered fashion to form the image of the "microtrabecular lattice." In their comparison of detergent-extracted and whole, unextracted cells, Heuser and Kirschner (15) basically made the same observation but reached a different conclusion. They favor the view that microtrabeculae are "a different sort of image of the same cytoskeletal filaments" (p. 233), whereas, in our opinion, there exists a filamentous system of probably heteregeneous biochemical composition superimposed upon the Triton-extracted cytoskeleton. This conslusion is based in part on the analysis of images such as those shown in Figs. 15 and 16 and also on additional work (27) that bears more directly on the reality of the microtrabecular network described by Wolosewick and Porter (44, 45).

In summary, the Triton-extracted residue appears as a highly crosslinked structural unit and not just a tangle of numerous filaments. One could easily travel across a cell along fibrous structures and yet change the "carrier" filament several hundred times. Due to this extensive "crosstalking" between the major components of the cytoskeleton, experiments designed specifically to affect one component will most certainly influence the structural organization of other components as well. For example, cytochalasin-induced filament rearrangements also have an effect on microtubule organization (Fig. 14); other examples have been described in the literature (e.g., references 9, 10). With our technique, we are now in a position

to monitor cytoskeletal changes associated with different activities of the cell or reactions to drug treatments. In addition, we can proceed to localize, at the electron microscopic level, important components associated with the cytoskeleton, such as α-actinin, myosin, or filamin. Such studies have already been initiated.

REFERENCES

1. Allen, N. S. 1980. Cytoplasmic streaming and transport in the characean alga *Nitella. Can. J. Bot.* 58:786–796.
2. Batten, B. E., J. J. Aalberg, and E. Andersen. 1980. The cytoplasmic filamentous network in cultured ovarian granulosa cells. *Cell.* 21:885–895.
3. Ben-Ze'ev, A., A. Duerr, F. Solomon, and S. Penman. 1979. The outer boundary of the cytoskeleton: a lamina derived from plasma membrane proteins. *Cell.* 17:859–865.
4. Brinkley, B. R., S. H. Fistel, D. M. Marcum, and R. L. Pardue. 1980. Microtubules in cultured cells: indirect staining with tubulin antibody. *Int. Rev. Cytol.* 63:59–96.
5. Brown, S., W. Levinson, and J. Spudich. 1976. Cytoskeletal elements of chick embryo fibroblasts revealed by detergent extraction. *J. Supramol. Struct.* 5:119–130.
6. Buckley, I. K. 1975. Three-dimensional fine structure of cultured cells: possible implications for subcellular motility. *Tissue & Cell.* 7:51–72.
7. Buckley, I. K., and K. R. Porter. 1975. Electron microscopy of critical point dried cultured cells. *J. Microsc. (Oxf.)* 104:107–120.
8. Fujiwara, K., and T. D. Pollard. 1978. Simultaneous localization of myosin and tubulin in tissue culture cells by double antibody staining. *J. Cell Biol.* 77:182–195.
9. Goldman, R. D. 1971. The role of three cytoplasmic fibers in BHK-21 cell motility. I. Microtubules and the effects of colchicine. *J. Cell Biol.* 51:752–762.
10. Gordon, W. E., A. Bushnell, and K. Burridge. 1978. Characterization of the intermediate (10 nm) filaments of cultured cells using an autoimmune rabbit antiserum. *Cell.* 13:249–261.
11. Griffith, L. M., and T. D. Pollard. 1978. Evidence for actin filament—microtubule interaction mediated by microtubule-associated proteins. *J. Cell Biol.* 78:958–965.
12. Groeschel-Stewart, U. 1980. Immunochemistry of cytoplasmic contractile proteins. *Int. Rev. Cytol.* 65:193–254.
13. Hartwig, J. H., J. Tyler, and T. P. Stossell. 1980. Actin binding protein promotes the bipolar and perpendicular branching of actin filaments. *J. Cell Biol.* 87:841–848.
14. Henderson, D., and K. Weber. 1979. Three dimensional organization of microfilaments and microtubules in the cytoskeleton. *Exp. Cell Res.* 124:301–316.
15. Heuser, J. E., and M. W. Kirschner. 1980. Filament organization revealed in platinum replicas of freeze-dried cytoskeletons. *J. Cell Biol.* 86:212–234.
16. Ip, W., and D. A. Fishman. 1979. High resolution scanning electron microscopy of isolated and *in situ* cytoskeletal elements. *J. Cell Biol.* 83:249–254.
17. Kirschner, M. W. 1980. Implications of treadmilling for the stability and polarity of actin and tubulin polymers in vivo. *J. Cell Biol.* 86:330–334.
18. Lenk, R., L. Ransom, Y. Kaufman, and S. Penman. 1977. A cytoskeletal structure with associated polyribosomes obtained from HeLa cells. *Cell.* 10:67–78.
19. Maruyama, K., M. Kaibara, and F. Fukuda. 1974. Rheology of F-actin. I. Network of F-actin in solution. *Biochim. Biophys. Acta.* 371:20–29.
20. O'Farrell, P. H. 1975. High resolution two-dimensional electrophoresis of proteins. *J. Biol. Chem.* 250:4007–4021.
21. Osborn, M., and K. Weber. 1977. The detergent-resistant cytoskeleton of tissue culture cells includes the nucleus and the microfilament bundles. *Exp. Cell Res.* 106:339–349.
22. Osborn, M., T. Born, H. J. Koitzsch, and K. Weber. 1978. Stereo immunofluorescence microscopy. I. Three dimensional arrangement of microfilaments, microtubules, and tonofilaments. *Cell.* 14:477–488.
23. Pudney, J., and R. H. Singer. 1979. Electron microscopic visualization of filamentous reticulum in whole cultured presumptive chick myoblasts. *Am. J. Anat.* 156:321–336.
24. Schiff, P. B., J. Fant, and S. B. Horowitz. 1979. Promotion of microtubule assembly *in vitro* by Taxol. *Nature (Lond.).* 277:665–667.
25. Schliwa, M. 1980. Structural organization of detergent-extracted cells. Proceedings of the

26. Schliwa, M., and J. van Blerkom. 1980. Three-dimensional organization and interaction of cytoskeletal structures. *Eur. J. Cell Biol.* 22:352 (Abstr.).
27. Schliwa, M., J. van Blerkom, and K. R. Porter. 1981. Stabilization of the cytoplasmic ground substance in detergent-opened cells, and a structural and biochemical analysis of its composition. *Proc. Natl. Acad. Sci. U. S. A.* In press.
28. Schliwa, M., U. Euteneuer, J. C. Bulinski, and J. G. Izant. 1981. Calcium lability of cytoplasmic microtubules and its modulation microtubule-associated proteins. *Proc. Natl. Acad. Sci. U. S. A.* 78:1037–1041.
29. Shelanski, M. L., F. Gaskin, and C. R. Cantor. 1973. Microtubule assembly in the absence of added nucleotides. *Proc. Natl. Acad. Sci. U. S. A.* 70:765–768.
30. Small, J. V., and J. E. Celis 1978. Direct visualization of the 10-nm (100 Å) filament network in whole and enucleated cultured cells. *J. Cell Sci.* 31:393–409.
31. Small, J. V., and A. Sobieszek. 1977. Studies on the function and composition of the 10-nm (100 Å) filaments of vertebrate smooth muscle. *J. Cell Sci.* 23:243–268.
32. Summers, K., and M. W. Kirschner. 1979. Characteristics of the polar assembly and disassembly of microtubules observed in vitro by dark-field light microscopy. *J. Cell Biol.* 83:205–217.
33. Telzer, B. R., and J. L. Rosenbaum. 1980. Cell-cycle dependent, in vitro assembly of microtubules onto the pericentriolar material of HeLa cells. *J. Cell Biol.* 81:484–501.
34. Temmick, J. H. M., and H. Spiele. 1978. Preservation of cytoskeletal elements for electron microscopy. *Cell Biol. Int. Rep.* 2:51–59.
35. Tilney, L. G., D. de Rosier, and M. J. Mulroy. 1980. The organization of actin filaments in the stereocilia of cochlear hair cells. *J. Cell Biol.* 86:244–259.
36. Trotter, J. A., B. A. Foerder, and J. M. Keller. 1978. Intracellular fibers in cultured cells: analysis by scanning and transmission electron microscopy and by SDS-polyacrylamide gel electrophoresis. *J. Cell Sci.* 31:369–392.
37. van Blerkom, J. 1978. Methods for the high resolution analysis of protein synthesis: applications to early mammalian development. *In* Methods in Mammalian Reproduction, J. C. Daniel, editor, Academic Press, Inc., New York. 67–109.
38. Weber, K., and M. Osborn. 1979. Intracellular display of microtubular structures revealed by indirect immunofluorescence microscopy. *In:* Microtubules, K. Roberts and J. S. Hyams, editors. Academic Press, Inc. London. 279–314.
39. Weber, K., P. C. Rathke, and M. Osborn. 1978. Cytoplasmic microtubular images in glutaraldehyde-fixed tissue culture cells by electron microscopy and by immunofluorescence microscopy. *Proc. Natl. Acad. Sci. U. S. A.* 75:1820–1824.
40. Webster, R. E., M. Osborn, and K. Weber. 1978. Visualization of the same PtK₂ cytoskeletons by both immunofluorescence and low power electron microscopy. *Exp. Cell Res.* 117:47–61.
41. Webster, R. E., D. Henderson, M. Osborn, and K. Weber. 1978. Three-dimensional electron microscopical visualization of the cytoskeleton of animal cells: immunoferritin identification of actin- and tubulin-containing structures. *Proc. Natl. Acad. Sci. U. S. A.* 75:5511–5515.
42. Weeds, A. G., and R. S. Taylor. 1975. Separation of subfragment 1-isoenzymes from rabbit skeletal muscle myosin. *Nature (Lond.).* 257:54–56.
43. Wieland, T. 1977. Modification of actins by phallotoxins. *Naturwissenschaften.* 64:303–309.
44. Wolosewick, J. J., and K. R. Porter. 1976. Stereo high voltage electron microscopy of whole cells of the human diploid cell line WI-38. *Am. J. Anat.* 147:303–324.
45. Wolosewick, J. J., and K. R. Porter. 1979. Microtrabecular lattice of the cytoplasmic ground substance. Artifact or reality. *J. Cell Biol.* 82:114–139.
46. Woodrum, T. T., S. A. Rich, and T. D. Pollard. 1975. Evidence for the biased bidirectional polymerization of actin using heavy meromyosin produced by an improved method. *J. Cell Biol.* 67:231–237.

38th Meeting of Electron Microscopy Society of America. G. W. Bailey, editor. Claitors Publishing Division, Baton Rouge, La. 814–817.